Differential bortezomib sensitivity in head and neck cancer lines corresponds to proteasome, nuclear factor-κB and activator protein-1 related mechanisms

Zhong Chen,[1] Justin L. Ricker,[1] Pramit S. Malhotra,[2] Liesl Nottingham,[1] Lorena Bagain,[1] Tin Lap Lee,[1] Ning T. Yeh,[1] and Carter Van Waes[1]

[1]Tumor Biology Section, Head and Neck Surgery Branch, National Institute on Deafness and Other Communication Disorders, NIH, Bethesda, Maryland and [2]Department of Otolaryngology-Head and Neck Surgery, University of Minnesota Hospitals, Minneapolis, Minnesota

Abstract

Head and neck squamous cell carcinomas (HNSCC) exhibit constitutive activation of transcription factors nuclear factor-κB (NF-κB) and activator protein-1 (AP-1), which are modulated by the proteasome and promote resistance to cell death. HNSCC show variable sensitivity to the proteasome inhibitor bortezomib *in vitro* as well as in murine xenografts and patient tumors *in vivo*, and the mechanisms are not well understood. To address this question, the sensitivities of nine HNSCC cell lines to bortezomib were determined using 3-(4,5-dimethylthiazol-2-yl)-2,5-diphenyltetrazolium bromide assays, and the potential relationship between the sensitivity and bortezomib effects on biological processes was examined in HNSCC lines of differential bortezomib sensitivity. The most sensitive cell line (UM-SCC-11B) underwent cell death at 10^{-9} mol/L *in vitro* and tumor regression at a maximally tolerated dose of bortezomib in a murine xenograft model. The differential sensitivity between UM-SCC-11A and UM-SCC-11B cells corresponded to differences in the extent of suppression of proteasome activity, ubiquitinated protein degradation, and NF-κB and AP-1 activation. Lower concentrations of bortezomib transiently increased NF-κB and sustained AP-1 activation in UM-SCC-11A cells. AP-1 reporter activity and cell density of UM-SCC-11A were suppressed when bortezomib was combined with c-Jun NH_2-terminal kinase and p38 kinase pathways inhibitors. Thus, the differential sensitivities to bortezomib corresponded to dissimilar effects on the proteasome, NF-κB and AP-1 activities. Inhibition of c-Jun NH_2-terminal kinase and p38 pathways blocked AP-1 activity and enhanced the antitumor effects. These findings revealed molecular mechanisms of bortezomib sensitivity and resistance, which are under development as biomarkers for clinical trials in patients with HNSCC. [Mol Cancer Ther 2008;7(7):1949–60]

Introduction

Constitutive activation of the nuclear factor-κB (NF-κB) and activator protein-1 (AP-1) signal transduction pathways have been identified as prominent events promoting tumor progression of hemopoietic and solid malignancies (1–4), including head and neck squamous cell carcinomas (HNSCC; refs. 5–7). We have shown that NF-κB is frequently coactivated with AP-1 and promotes the proliferative, prosurvival, and proangiogenic cancer phenotype (6, 7). Targeting NF-κB and AP-1, or upstream signal transduction pathways by genetic or chemical inhibitors, has been shown to effectively suppress the tumor phenotype *in vitro* as well as inhibit tumor growth in preclinical animal models and patient tumors *in vivo* (4, 5, 7–11). Subsequent clinical studies have correlated NF-κB and AP-1 pathways, as well as their targeted biomarkers, with worse prognosis (12–15). Thus, aberrant activation of NF-κB and AP-1 are critical signal transduction pathways promoting the aggressive tumor phenotype and survival of HNSCC.

Bortezomib (Velcade/PS-341) has been developed in recent years for molecular targeting and inhibition of the proteasome, a complex that mediates the turnover of many intracellular proteins, including those controlling cell signaling, survival, and cell cycle regulation (16, 17). Bortezomib selectively inhibits proteasome activity, which is required for activation of NF-κB and degradation of components of AP-1 and other signal pathways involved in the pathogenesis of cancer (16–18). Bortezomib can inhibit the NF-κB pathway through its inhibitory effects on degradation of ubiquitinated inhibitor κB (IκB), which binds and sequesters NF-κB in the cytoplasm, inhibiting its nuclear localization and binding to the promoters of target genes (11, 16, 17, 19–21). The protein components of AP-1 family members are also degraded through the proteasome

Received 9/11/07; revised 3/25/08; accepted 4/1/08.

Grant support: National Institute on Deafness and Other Communication Disorders intramural project Z01-DC-00016.

The costs of publication of this article were defrayed in part by the payment of page charges. This article must therefore be hereby marked *advertisement* in accordance with 18 U.S.C. Section 1734 solely to indicate this fact.

Note: Bortezomib was provided for research under a Materials Cooperative Research and Development Agreement with Millennium Pharmaceuticals.

Requests for reprints: Carter Van Waes, Tumor Biology Section, Head and Neck Surgery Branch, National Institute on Deafness and Other Communication Disorders, NIH, 10/5D55, MSC-1419, Bethesda, MD 20892-1419. Phone: 301-402-4216; Fax: 301-402-1140. E-mail: vanwaesc@nidcd.nih.gov

doi:10.1158/1535-7163.MCT-07-2046

system (18, 21). The inhibitory activity of bortezomib has been shown against a spectrum of cancer cells in culture (11, 19–29) and in animal models (11, 30–32), including suppression of NF-κB and other signal transcription pathways (11, 16, 17, 19–25, 27, 34), with induction of cell apoptosis and cell cycle arrest (19, 20, 22–35). The molecular and clinical effects of bortezomib and potential mechanisms of variable activity have been most extensively studied in multiple myeloma and certain other hematopoietic malignancies (20, 22–25, 33–35) but to a lesser extent in solid cancers (8, 11, 19, 26–32). In clinical trials of carcinomas and solid tumors, lower response rates and greater heterogeneity in responsiveness to bortezomib monotherapy was observed compared with multiple myeloma (36–38), and combination of bortezomib with other anticancer agents has been undertaken in an effort to achieve significant anticancer effects *in vivo* (8, 37, 39).

Bortezomib shows antitumor and radiosensitizing effects in HNSCC cell lines and SCC animal models, which exhibit constitutively activated NF-κB (4–11, 32), and these responses are associated with inhibition of NF-κB, its target genes and expected cytopathic effects (11, 32). The antitumor effects of bortezomib against HNSCC *in vitro* and in murine models, and its suppressive effects against radiation-induced NF-κB activation (39), led us to develop a phase I clinical trial to investigate the optimal dose, schedule, toxicity, and antitumor effects of combination therapy of bortezomib and radiation in patients with HNSCC. In this trial, heterogeneity in response to the combination therapy has also been observed, with 5 of 17 evaluable patients treated to date showing objective responses (8).[3] Identification of molecular mechanisms for these differences in sensitivity, and markers for selection of therapy with bortezomib and/or additional agents, is desirable.

In this study, we identified a bortezomib-sensitive cell line, UM-SCC-11B, and a cell line of isogenic origin from the same patient, UM-SCC-11A, which showed relatively less sensitivity to bortezomib, similar to other members of a nine UM-SCC line panel. Between the two cell lines, we observed significant differences in their response to treatment in terms of proteasome inhibition, accumulation of ubiquitinated proteins, and corresponding effects on activation of transcription factors NF-κB and AP-1. Activation of AP-1 inhibited by c-Jun NH_2-terminal kinase (JNK) and p38 antagonists sensitized the more resistant line to the effects of bortezomib. These findings suggest that differences in proteasome-dependent effects on NF-κB and AP-1 may contribute to the differential sensitivity of HNSCC to bortezomib. Understanding such molecular differences involved in the cellular responses to bortezomib could provide biomarkers to guide us in improving the selection and potential combinations of treatment to be used with bortezomib.

Materials and Methods

HNSCC Lines

Human UM-SCC cell lines were derived from patients with SCC arising from sites in the upper aerodigestive tract at the University of Michigan, following informed consent, as described previously (Supplementary Table S1;[4] refs. 40, 41). The cell lines established from each patient specimen are designated by a numeric designation, and where isolates from two different time points or anatomical sites were obtained from the same patient, the designation includes an alphabetical suffix (''A'' or ''B''). The cell lines used were maintained in Eagle's MEM supplemented with 10% fetal bovine serum and penicillin/streptomycin.

Reagents

Proteasome inhibitor bortezomib was obtained from Millennium Pharmaceuticals under a Materials Cooperative Research and Development Agreement (8, 11). Tumor necrosis factor-α was purchased from R&D Systems. Rabbit polyclonal antibodies against β-tubulin (sc-9104), ubiquitin (sc-9133), and goat anti-rabbit IgG-horseradish peroxidase (sc-2004) were purchased from Santa Cruz Biotechnology. The chemical inhibitor for JNK, SP600125, was obtained from Biomol; the p38 inhibitor, SB203580, was obtained from Calbiochem/EMD Biosciences; and the inhibitors for MEK, UO126 and PD98059, were obtained from Promega and Calbiochem/EMD Biosciences, respectively.

Measurement of Cell Proliferation and Viability by Trypan Blue Exclusion

Cell proliferation was assessed by 3-(4,5-dimethylthiazol-2-yl)-2,5-diphenyltetrazolium bromide (MTT) assay. Cells (5×10^3) were plated in a 96-well microtiter plate in quadruplicates and treated by bortezomib the next day. MTT labeling reagent (Boehringer Mannheim) was added on days 1, 3, and 5 after treatment, and colorimetric absorbance was measured at 570 nm by a microplate autoreader (Biotek). For trypan blue exclusion assay, 2×10^5 UM-SCC-11A cells and 3×10^5 UM-SCC-11B cells were plated in T-25 flask and exposed to bortezomib 48 h after plating. Cells were harvested, stained with trypan blue dye, and visually counted under microscope at different time points.

Apoptosis and Cell Cycle Analysis by Flow Cytometry

UM-SCC-11A and UM-SCC-11B cells were plated in T-25 flask and treated with bortezomib at different concentrations as indicated. Cells were harvested at 12, 24, and 96 h after treatment and 10^5 cells were collected for DNA cell cycle and apoptosis analysis using cycleTEST Plus DNA reagent kit (Becton Dickinson). Cellular DNA was labeled with propidium iodide, and DNA content of 10,000 cells in each sample was measured by flow cytometry (FACScan; Becton Dickinson). Percentage of apoptotic and viable cells in each phase of cell cycle were analyzed by ModFit LT software (Verity Software House).

[3] C. Van Waes, unpublished data.

[4] Supplementary material for this article is available at Molecular Cancer Therapeutics Online (http://mct.aacrjournals.org/).

SCC Xenograft Tumor Model

BALB/c severe combined immunodeficient mice (4-6 weeks old) were obtained from the National Cancer Institute, Frederick Cancer Research and Development Center, and housed in a pathogen-free animal facility. UM-SCC-11A or UM-SCC-11B cells (1.5×10^7) were injected s.c. over the flanks of immunodeficient BALB/c severe combined immunodeficient mice (11, 32). When ~ 0.3 cm^3 palpable tumors were developed, 2.0 mg/kg/dose bortezomib (maximum tolerated dose tested previously) was administered by i.p. injections on a Monday/Wednesday/Friday schedule weekly for a total of three doses. Tumor size was measured weekly with an engineer caliper by an independent animal care personnel and presented as tumor volume that resulted from 2 (tumor width) $\times$ tumor length.

Terminal Deoxynucleotidyl Transferase–Mediated dUTP Nick End Labeling

SCC xenograft tumor specimens were harvested at different time points after bortezomib treatment, and thin frozen sections were processed by American Histo Lab. Terminal deoxynucleotidyl transferase–mediated dUTP nick end labeling (TUNEL) assay was carried on the specimens according to the manufacturer's instructions (Chemicon International).

Measurement of Proteasome Activity

Proteasome activity was measured according to the protocol by Elliott et al. (42). Protein lysate (10 μg) was incubated with the synthetic peptide substrate LLVY-AMC (Bachem) in each well of the 96-well plate in triplicates, and the release of the fluorophore AMC was measured by Wallac Victor^2 1420 multilabel counter at 37°C (λ_{ex} = 380 nm and λ_{em} = 450 nm). The kinetics of proteasome inhibitory activity was measured for five repetitive times after 10-s shaking and 4-min incubation.

NF-κB Binding Activity

To detect NF-κB p65 binding activity, cell nuclear extracts were obtained using Nuclear Extraction kit (Active Motif). Nuclear extracts (10 μg) were used in each reaction in triplicates. The binding activity was evaluated using TransAM kits for NF-κB family members according to manufacturer's protocol (Active Motif). The absorbance was measured at wavelength of 450 nm by a microplate reader (Biotek).

Reporter Gene Assays

5XNF-κB-luciferase and 7XAP-1-luciferase reporter gene constructs were purchased from Stratagene. Murine dominant-negative IκBαM plasmid (pCMX IκBαM) was kindly provided by Dr. Inder M. Verma (Salk Institute; ref. 7). Cells were plated at 5×10^4 per well in a 24-well plate in triplicates and the next day were transfected with 0.3 μg plasmid DNA plus Effectene Transfection Reagents for 3 h at 37°C following manufacturer's suggestions (Qiagen). After transfection, the cells were grown in Eagle's MEM plus 10% fetal bovine serum and exposed to bortezomib. The cell lysates were harvested and reporter gene activities were assayed using the Dual-Light Luciferase Reporter Gene Assay System (Tropix). The chemiluminescence activity was measured by a Monolight 2010 luminometer (Analytical Luminescence Lab).

Isolation of Whole-Cell Extract

Cells were plated in 100-mm tissue culture dishes and allowed to grow until 80% to 90% confluent, and the whole-cell lysates were isolated using nuclear extract kit (Active Motif). Cultured cells were washed with ice-cold PBS/phosphatase inhibitors and scraped and then were lysed in 100 μL lysis buffer and pipetted up and down several times. The lysates were incubated for 10 min on ice followed by centrifuged at 14,000 $\times$ g for 20 min at 4°C, and the supernatants were collected and stored at -80°C. Total protein concentrations were determined using the Pierce BCA protein assay method.

Western Blot Analysis

Whole-cell lysates (20 μg) were mixed with Laemmli loading buffer (containing β-mercaptoethanol) and heated at 100°C for 5 min. The samples were loaded onto 10% Tris-glycine precast gels and electrophoresed at 140 V for 90 min. The proteins were transferred to 0.45 μm nitrocellulose membranes (Invitrogen) for 2 h at 20 V at room temperature using the Invitrogen Gel Blot Module. Immunoblotting was conducted according to manufacturer's specifications. Primary antibodies were diluted in 5% nonfat powdered milk prepared from TBS-Tween 20 and diluted at 1:500, and the secondary goat anti-rabbit IgG-horseradish peroxidase was used at 1:1,000 dilution. Each blot was incubated with Pierce Super Signal West Pico substrate and exposed to Kodak X-OMAT film.

Results

Differences in Sensitivity of UM-SCC Cell Lines to Bortezomib

We screened nine UM-SCC cell lines and normal human keratinocytes for their sensitivity to bortezomib by MTT cell proliferation assay and identified UM-SCC-11B as the most sensitive cell line (Fig. 1A; Supplementary Table S1).[4] The IC_{50} value for bortezomib in UM-SCC-11B was 0.37 nmol/L, whereas a modest sensitivity was observed among cell lines, UM-SCC-1, UM-SCC-5, UM-SCC-6, UM-SCC-11A, UM-SCC-22A and UM-SCC-22B, where the IC_{50} values were $\sim$0.54 to 1.1 nmol/L. The most resistant cell lines identified were UM-SCC-9 and UM-SCC-38, where the IC_{50} values were 7.19 and 8.37 nmol/L. Although UM-SCC-11B and the other UM-SCC studied showed greater activation and dependence on NF-κB activation than UM-SCC-9, the degree of sensitivity to bortezomib among the cell lines was not strictly proportional to NF-κB activation (Fig. 1B; refs. 6, 7, 43), suggesting that other factors could contribute to the differential sensitivity observed. Cultured human normal keratinocytes also showed a relatively low IC_{50} (0.48 nmol/L), which was comparable with the tumor cells, while exhibiting minimal activation of NF-κB in culture (43).

To further investigate the potential mechanisms of the differential sensitivity of UM-SCC cell lines to bortezomib, we elected to study separate isolates of the same primary

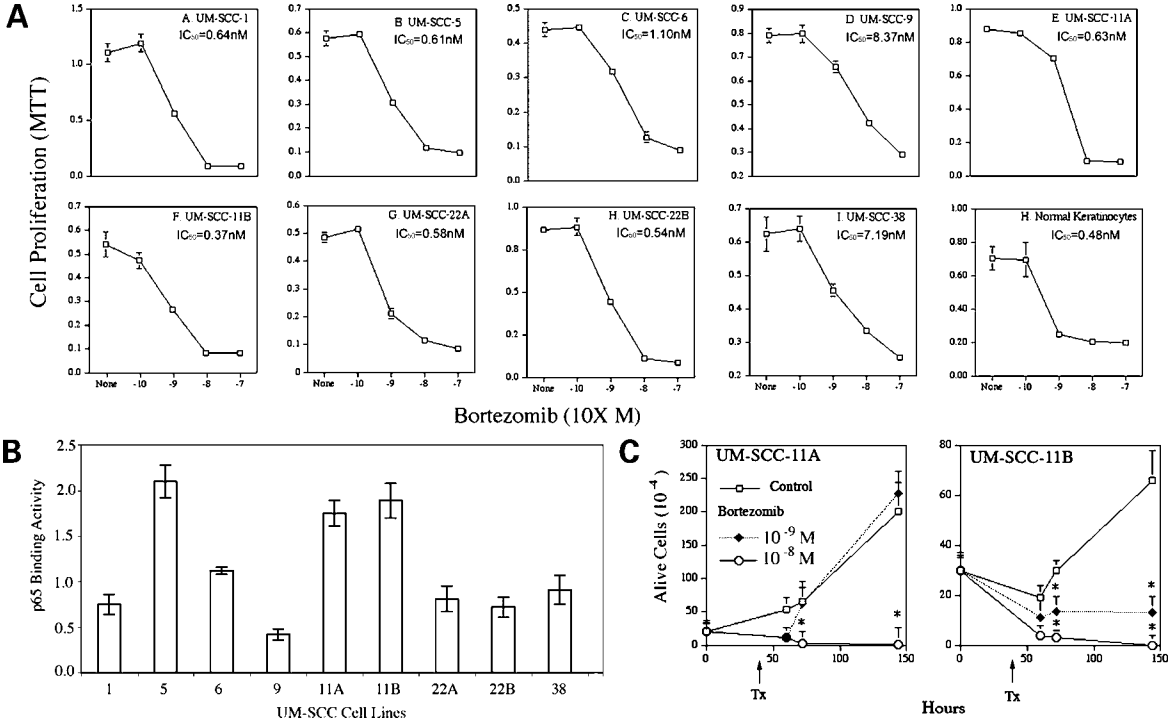

Figure 1. Sensitivity of UM-SCC cell lines and cultured normal human keratinocytes to bortezomib *in vitro*. **A,** nine UM-SCC cell lines and human normal keratinocytes were plated at 5×10^3 cells per well in quadruplicates in a 96-well microplate. The next day, cells were exposed to bortezomib at different concentrations (day 0). Cells were labeled with MTT reagent for 4 h at days 1, 2, and 3 after treatment, and the absorbance of labeled cells was measured the following day. Representative of repeated experiments showing mean ± SD from quadruplicates. The IC_{50} shown was calculated using the data from day 2. **B,** nuclear extracts were harvested from cultured UM-SCC cells, and NF-κB p65 binding activity was measured using a TransAM NF-κB binding kit with 10 μg nuclear extract in each well. Mean ± SD from triplicates. **C,** cytotoxic effects of bortezomib in UM-SCC-11 A and UM-SCC-11B cells were tested by trypan blue assay. UM-SCC-11A (*left*) and UM-SCC-11B cells (*right*) were plated in the T-25 flask in triplicates and treated with bortezomib at 10^{-9} and 10^{-8} mol/L 48 h later. At the each time point, both attached and detached cells were collected, stained with trypan blue dye, and counted. Total viable cells were calculated and presented.

hypopharyngeal HNSCC, which, interestingly, showed different alterations in sensitivity to bortezomib and other agents before (UM-SCC-11A) and after chemotherapy with cisplatin (UM-SCC-11B; Supplementary Table S1;[4] refs. 40, 41). After cisplatin chemotherapy, UM-SCC-11B cells showed elevated constitutive and epidermal growth factor induced NF-κB and STAT3 levels, and resistance to epidermal growth factor receptor inhibitor, gefitinib (7, 44, 45), but greater sensitivity to bortezomib *in vitro* and in murine xenografts (11). When we compared the cell viability of the two cell lines by trypan blue exclusion assay after treatment with bortezomib, we confirmed our previous observation that UM-SCC-11B cells were more sensitive to bortezomib than UM-SCC-11A cells in terms of induction of cytotoxicity and reduction of viable cells (Fig. 1C).

Antitumor Activity of Bortezomib *In vivo*

The antitumor activity of bortezomib in UM-SCC-11A and UM-SCC-11B was further evaluated in a xenograft tumor model in severe combined immunodeficient mice (11, 32). A HNSCC xenograft tumor model established by s.c. injection of tumor cells was used in this study to examine the potential differences in response to bortezomib, as the rate of growth of tumors when implanted orthotopically causes premature death due to obstruction of swallowing or respiration. However, this model represents many molecular characteristics similar to other HNSCC xenografts implanted in orthotopic murine models (46). At maximal tolerated doses, we observed tumor regression of UM-SCC-11B tumors after three injections (Fig. 2A, *right*) but no effect on UM-SCC-11A tumors (Fig. 2A, *left*). Tumor specimens were also harvested after bortezomib treatment. Bortezomib treatment induced UM-SCC-11B tumor cell nuclear condensation and tissue degradation (Fig. 2B, *top right*), as well as TUNEL labeling consistent with apoptosis (Fig. 2B, *bottom right*), when compared with the vehicle controls (Fig. 2B, *left*). However, the morphology of UM-SCC-11A tumors after treatment were the same as the vehicle controls, and there was no TUNEL labeling observed in the UM-SCC-11A tumor samples treated with bortezomib (data not shown).

Bortezomib Induced Cell Cycle Blockade in UM-SCC-11A Cells and Cell Apoptosis in UM-SCC-11B Cells

To further determine if bortezomib induced differential effects on cell cycle and/or apoptosis in UM-SCC-11A and UM-SCC-11B cells, DNA cell cycle analysis was done by flow cytometry. UM-SCC-11A cells treated with

10^{-8} mol/L bortezomib showed a significant cell cycle arrest in G_2-M phase between 12 and 24 h after treatment (Fig. 3A). In contrast, UM-SCC-11B cells, treated with the same concentration of bortezomib, showed a slight alteration of cell cycle distribution at 12 h and a markedly increased sub-G_0-G_1 DNA fragmentation peak within 24 h after treatment, consistent with apoptosis (Fig. 3B). At the lower concentration (10^{-9} mol/L), no significant cell cycle alteration or apoptosis were observed in UM-SCC-11A cells (Fig. 3A), but apparent changes of cell cycle were observed in UM-SCC-11B cells (Fig. 3B).

Differential Inhibition of Proteasome Activity by Bortezomib in UM-SCC-11A and UM-SCC-11B Cells

We next explored if the different sensitivity to bortezomib observed in UM-SCC-11A and UM-SCC-11B was potentially due to intrinsic differences in proteasome inhibition. We tested the proteasome activity in both cell lines after bortezomib treatment at different time points and found that strong inhibition was observed by 4 h after bortezomib treatment. As shown in Fig. 4, at a lower dose of bortezomib (10^{-9} mol/L), there was a slight but significant stimulation of proteasome activity in UM-SCC-11A cells but inhibition in UM-SCC-11B cells (Fig. 4A). At higher concentrations, we saw stronger inhibition of proteasome activity in UM-SCC-11B cells when compared with UM-SCC-11A cells (Fig. 4A). In addition, we examined the accumulation of ubiquitinated proteins, an effect of proteasome inhibition, in the two cell lines following treatment with 10^{-8} mol/L bortezomib at the different time points. More significant accumulation of ubiquitylated proteins was observed in UM-SCC-11B cells than in UM-SCC-11A cells (Fig. 4B), consistent with stronger proteasome

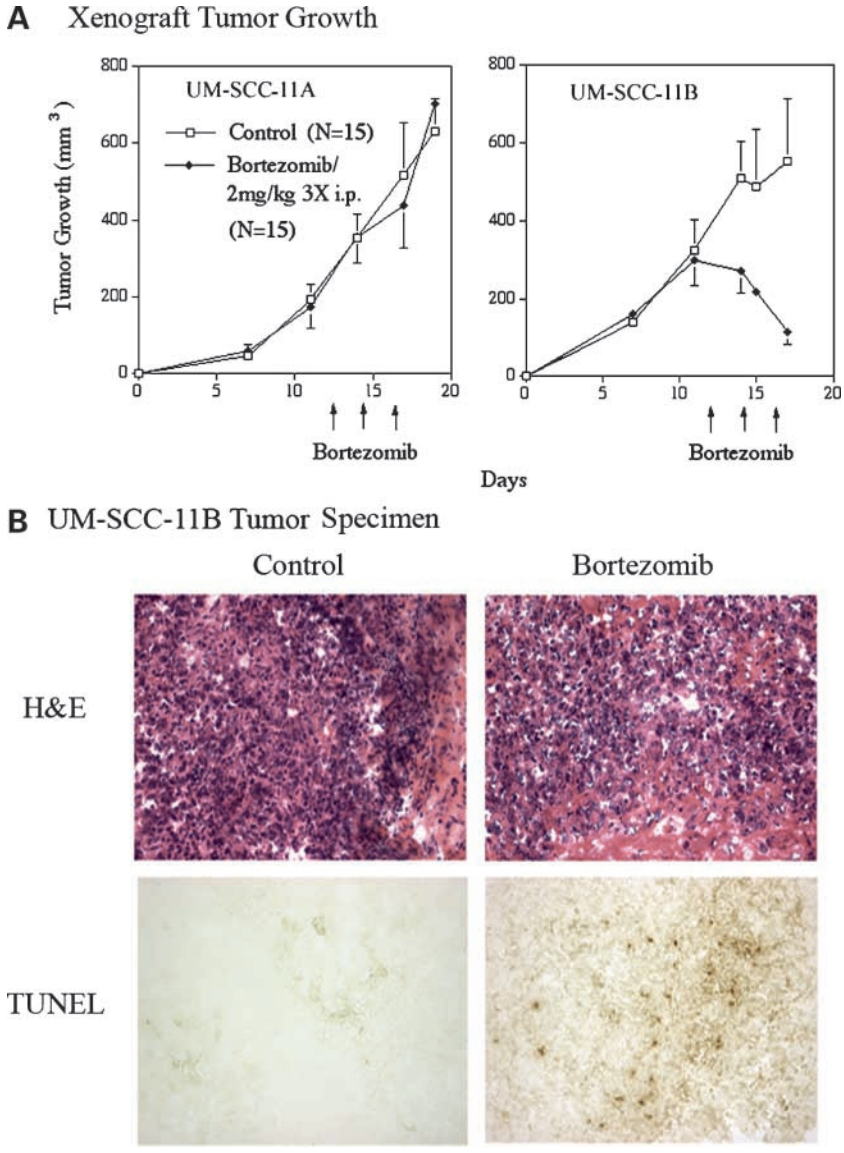

Figure 2. Antitumor activity of bortezomib in human UM-SCC tumor xenograft model. **A,** UM-SCC-11A and UM-SCC-11B cells were injected s.c. at the dosage of 1.5×10^7 per mouse over the flanks of immunodeficient BALB/c severe combined immunodeficient mice. When the mean tumor volume reached ~0.3 cm^3 in each tumor-bearing group, i.p. injections of bortezomib (2.0 mg/kg/dose) were administered on a Monday/Wednesday/Friday schedule. *Arrows,* time of each dose. Tumors were measured, and tumor volume was calculated. Mean ± SE. Vehicle for compound delivery was DMSO in sterile PBS. **B,** tumors from UM-SCC-11B xenograft models were harvested 24 h after bortezomib treatment, and H&E and TUNEL stainings were done on the frozen sections. The photographs of controls (*left*) and bortezomib-treated tumors (*right*) were taken under the light microscopy with ×200 magnification.

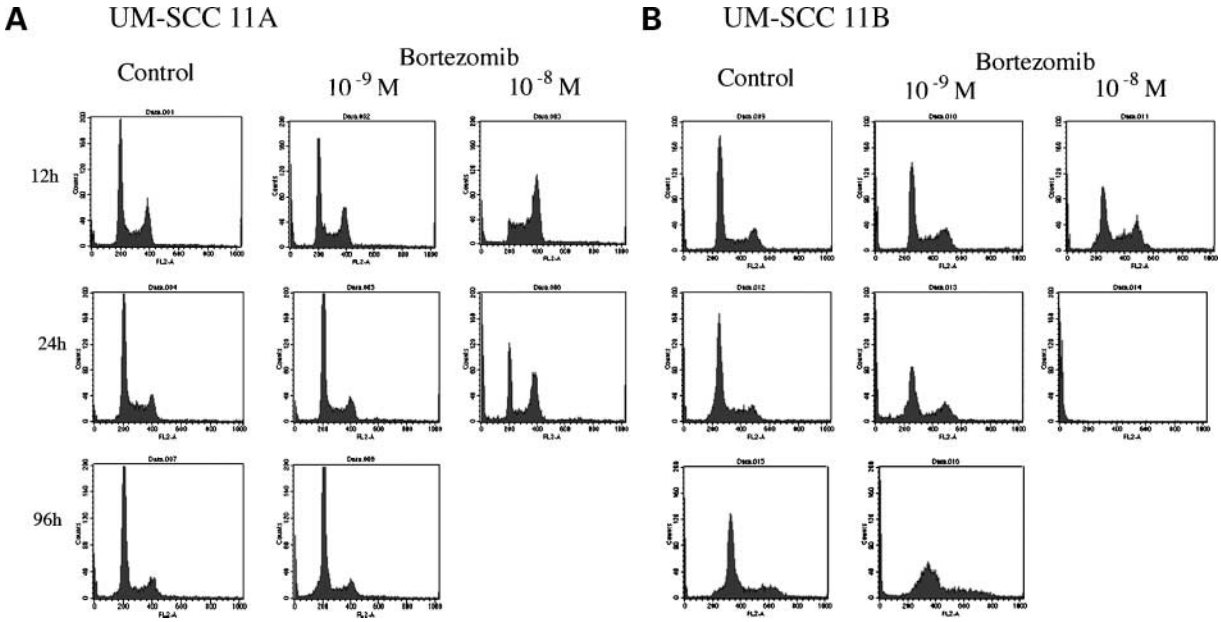

Figure 3. Bortezomib induced cell cycle arrest and apoptosis in UM-SCC-11A and UM-SCC-11B cells. UM-SCC-11A (**A**) and UM-SCC-11B (**B**) cells were treated with bortezomib at different concentrations and harvested at 12, 24, and 96 h after treatment. Cells (10^5) were collected and stained with propidium iodide for apoptosis and cell cycle analysis using cycleTEST Plus DNA reagent kit. Fluorescence intensity of 10,000 cells in each sample was measured by flow cytometry.

inhibition. Thus, UM-SCC-11A and UM-SCC-11B cells appear to exhibit differences in effect of bortezomib on proteasome inhibition and accumulation of ubiquitinated proteins.

Bortezomib Effects on NF-κB and AP-1 Activity

To explore if differences in sensitivity could reflect differences in NF-κB and/or AP-1 activation detected previously in HNSCC, we examined basal and bortezomib induced activity. UM-SCC-11A and UM-SCC-11B cells exhibited high basal levels of constitutively activated NF-κB as shown by NF-κB p65 binding (Fig. 1B) and reporter activities (Z. Chen, data not shown). UM-SCC-11A cells exhibited higher transfection efficiency and absolute luciferase activity than UM-SCC-11B cells; however, after normalization to β-gal activity, UM-SCC-11B showed 2-fold higher reporter activity than UM-SCC-11A cells (Z. Chen, data not shown), consistent with the difference in binding activity. To examine if the differential sensitivity to

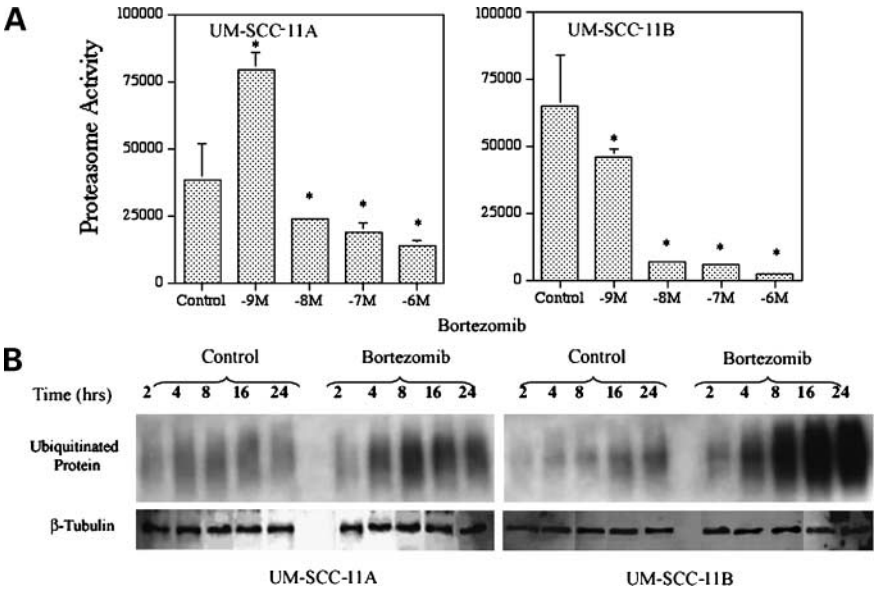

Figure 4. Bortezomib differentially inhibited the proteasome activity and protein ubiquitination in UM-SCC-11A and UM-SCC-11B cells. UM-SCC-11A (*left*) and UM-SCC-11B (*right*) cells were treated with bortezomib at different concentration, and the cell lysates were harvested 4 h after treatment. The proteasome activity was measured, and data were calculated and presented as the mean ± SD from the triplicates. *, indicates statistical significance compared with controls (*t*-test, $P < 0.05$). Cells were treated with bortezomib at 10^{-8} mol/L and the cell lysates were harvested at different time points. The protein ubiquitination was assessed by the Western blot analysis with anti-ubiquitin antibody (**B**).

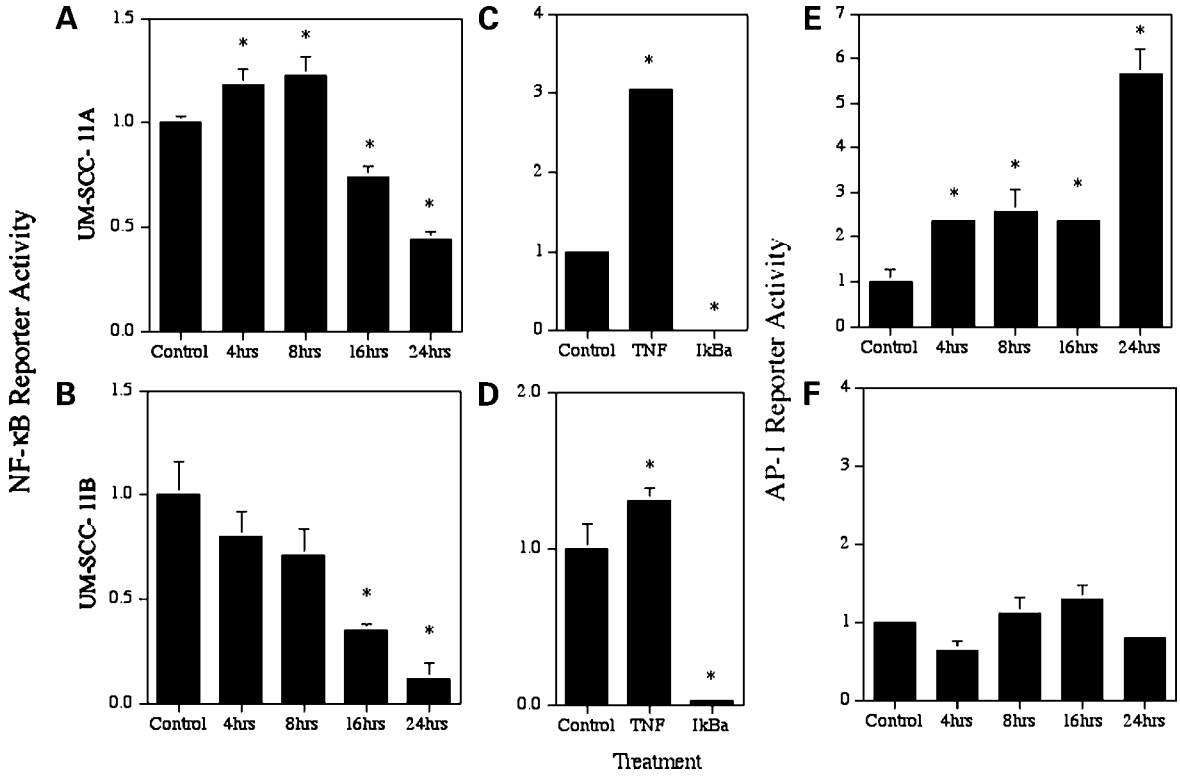

Figure 5. Bortezomib differentially affected NF-κB and AP-1 reporter activities in UM-SCC-11A and UM-SCC-11B cells. UM-SCC-11A and UM-SCC-11B cells were transiently transfected with NF-κB (**A – D**) or AP-1 (**E** and **F**) luciferase reporter constructs. After transfection, cells were treated with bortezomib at 10^{-8} mol/L for different time points. Cell lysates were harvested and analyzed for luciferase activity using Tropix Dual-Light reporter assay system. Each value were adjusted to controls and represented as the mean ± SD luciferase activity from triplicates. For the positive controls, the cells were also cotransfected with dominant-negative IκBαM plasmid with a NF-κB luciferase reporter construct and treated with 2,000 units/mL human recombinant tumor necrosis factor-α for 24 h (**C** and **D**). *, indicates statistical significance compared with controls (*t*-test, $P < 0.05$).

bortezomib observed in UM-SCC-11A and UM-SCC-11B cells was related to their NF-κB activity, NF-κB-luciferase reporter assays were conducted after cells were exposed to 10^{-8} mol/L bortezomib at different time points (Fig. 5). Bortezomib transiently increased NF-κB activity in UM-SCC-11A cells at the early time points (4 and 8 h after treatment) followed by relatively weaker NF-κB inhibition at 16 and 24 h after treatment (Fig. 5A). Bortezomib reduced NF-κB reporter activity in UM-SCC-11B cells by 4 h and reached statistical significance to nearly complete inhibition by 16 to 24 h after treatment (Fig. 5B). Next, we asked whether NF-κB activity in the cells could be stimulated and inhibited by the classic mechanisms, such as tumor necrosis factor-α, or overexpression of a dominant-negative IκBαM by transient transfection. In both cell lines, tumor necrosis factor-α was able to stimulate NF-κB reporter activity, and expression of the dominant-negative IκBαM was able to completely suppress NF-κB reporter activity (Fig. 5C and D).

Our laboratory previously identified another transcription factor AP-1, which is constitutively coactivated and promotes proliferation and the production of proangiogenic cytokines in HNSCC (6, 7). Because the induction of AP-1 occurs in response to many types of cellular stress, and degradation of proteins such as c-Jun that comprise AP-1 occurs via the proteasome (18), we tested if bortezomib affected AP-1 activity in these cells. As shown in Fig. 5E, bortezomib significantly increased AP-1 activity, as early as 4 h after treatment in UM-SCC-11A cells, but not in the UM-SCC-11B cells (Fig. 5F).

Blockade of Upstream Signaling Pathways Activating AP-1 Enhanced Bortezomib Effects in UM-SCC-11A Cells

We next examined if the constitutive and bortezomib-inducible AP-1 activity by bortezomib could contribute to the relative resistance of UM-SCC-11A cells. Because multiple signal transduction pathways upstream of AP-1 may contribute to AP-1 activation, several chemical inhibitors for these pathways were tested, including specific JNK inhibitor SP600125, p38 inhibitor SB203580, and MEK/extracellular signal-regulated kinase (ERK) inhibitors UO126 and PD98059 (27). We titrated these chemical inhibitors to suboptimum dosage for inhibition of MTT in UM-SCC-11A cells and combined them with bortezomib at 10^{-8} mol/L (Fig. 6A). We found the combination of bortezomib with JNK inhibitor SP600125 showed significant synergistic inhibitory effects on cell proliferation of UM-SCC-11A cells (Fig. 6A, *left*). Other inhibitors, such as

SB203580 for the p38 pathway (Fig. 6A, *right*) and UO126 and PD98059 for the ERK pathway, showed lesser combined activity (data not shown). Consistent with this, the combination of bortezomib and the JNK inhibitor SP600125 showed more significant inhibition on AP-1 reporter activity in UM-SCC-11A cells than either agent alone (Fig. 6B). Our data support the hypothesis that activation of JNK and AP-1 pathways could contribute to bortezomib resistance in UM-SCC-11A cells.

Discussion

In this study, sensitivity to bortezomib was determined in a panel of nine UM-SCC lines and cultured normal human keratinocytes, and the role of NF-κB and other potential mechanisms in bortezomib sensitivity were examined. The pharmacologic concentrations for the IC_{50} ranged between 0.37 and 8.37 nmol/L (Fig. 1), consistent with the range of sensitivities for other solid and hematopoietic malignancies (11, 19–28, 30–35) rather than the higher IC_{50} reported previously for HNSCC lines (29). Although UM-SCC-11B and most other UM-SCC cell lines studied exhibited greater NF-κB activation and bortezomib sensitivity than UM-SCC-9 and nonmalignant keratinocytes, the differential sensitivity to bortezomib among the cell lines in this study was not strictly proportional to the baseline differences in activation of NF-κB (Fig. 1B; ref. 6, 8, 43), indicating that other NF-κB-independent mechanism(s) potentially affected by proteasome inhibition may contribute to the differential sensitivities (16–18). Comparison of UM-SCC-11A and UM-SCC-11B cell lines isolated from the same patient before and after chemotherapy with cisplatin displayed different sensitivities and responses both *in vitro* and *in vivo* (Fig. 1; Supplementary Table S1),[4] suggesting that differences in mechanism(s) intrinsic to these cell lines could contribute to their differential sensitivities to bortezomib. Comparison of baseline and post-treatment levels of Bcl-2/Bcl-xL and Hsp27, previously implicated in intrinsic differences in sensitivity of multiple myeloma (25, 33), did not substantially differ between the lines (data not shown). Although UM-SCC-11A and UM-SCC-11B both showed similarly high levels of NF-κB activation, they displayed greater differences in the kinetics and extent of proteasome inhibition, ubiquitination, and AP-1 activation (Figs. 4 and 5). Inhibitors of JNK and p38 inhibited activation of AP-1 and sensitized cells to bortezomib (Fig. 6), indicating that bortezomib-induced signal activation of these kinase pathways both contribute to these differences in sensitivity and may serve as potential targets for combined therapy in HNSCC.

The difference in IC_{50} for bortezomib between UM-SCC-11A and UM-SCC-11B cells *in vitro* was less than 1 log

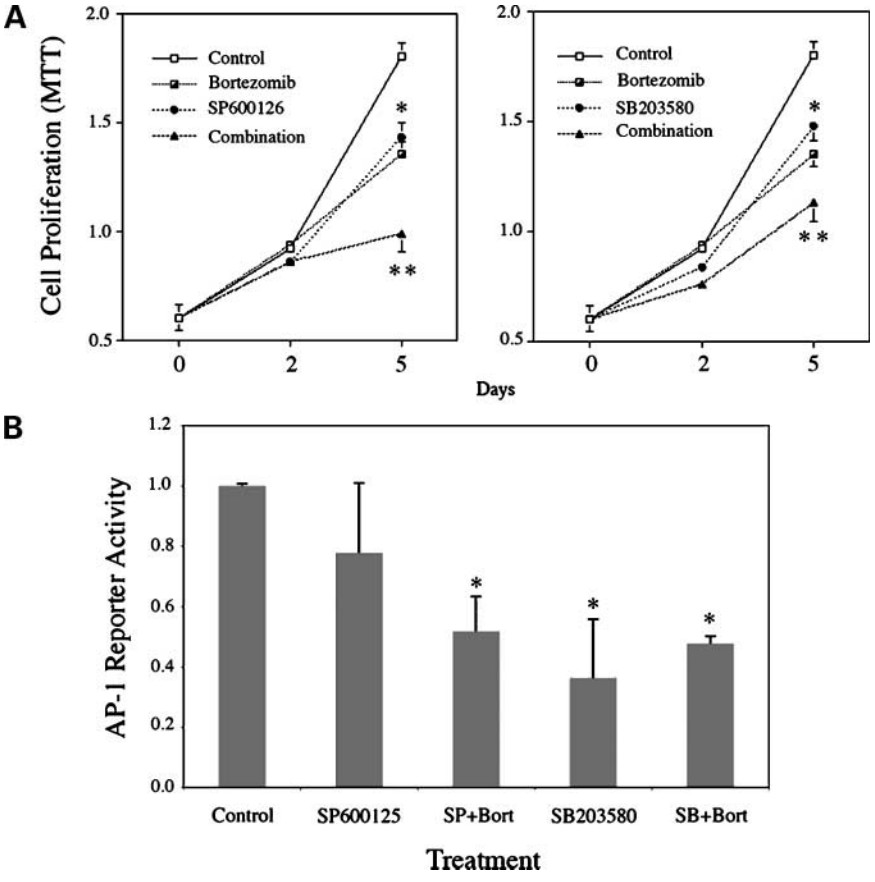

Figure 6. Chemical JNK inhibitor SP600125 significantly synergizes with bortezomib to inhibit cell proliferation and inhibits AP-1 reporter activity in UM-SCC-11A cells. **A,** UM-SCC-11A cells were plated in 96-well plates overnight, and chemical inhibitors were added 4 h before bortezomib treatment. Then cells were labeled with MTT reagent for 4 h at days 1, 3, and 5 after treatment, and absorbance of labeled cells was measured the following day. **B,** UM-SCC-11A cells were plated in 24-well plates overnight and transfected with AP-1 and LacZ reporter constructs. After transfection, the cells were treated with 10 μmol/L SP600125 or SB203580 for 4 h and then treated with 10^{-8} mol/L bortezomib for 24 h. The cells were harvested and reporter activity was measured as described previously. *, indicates significant inhibition by single agent, and **, indicates the significant inhibition by combined treatments compared with single agents (*t*-test, $P < 0.05$).

in the concentration range, but such a difference corresponded with a significantly altered drug activity for UM-SCC-11A or UM-SCC-11B xenograft tumor growth *in vivo* (Fig. 2A). At the maximally tolerated dosage in this preclinical xenograft tumor model, bortezomib induced UM-SCC-11B tumor regression (Fig. 2A) and cell apoptosis by TUNEL staining (Fig. 2B) but had no inhibitory effect on UM-SCC-11A tumors at the maximally tolerated dose (Fig. 2A; data not shown), indicating that such a dosage of bortezomib did not achieve sufficient intratumoral concentrations to induce regression of UM-SCC-11A tumors *in vivo*. Such differences in the response to bortezomib by the two cell lines *in vitro* and *in vivo* are consistent with differences in clinical responses in our ongoing phase I trial of combination therapy of bortezomib with reirradiation in patients with recurrent HNSCC (8, 47), where objective responses have been observed in a subset of 5 of 17 evaluable patients treated with 0.6 mg/m^2 with different schedules of reirradiation (8, 47). The limited responses observed in our clinical trial could partially be explained by the expected activity of the relatively low dose of bortezomib (0.6 mg/m^2), studied thus far with different schedules of reirradiation (8, 47), where the bortezomib serum concentration estimated from previous pharmacokinetic studies would fall in the lower concentration range (47–49). When limiting concentrations are present, increased interstitial pressures have been implicated in poorer bioavailability and relatively lower response rates in solid malignancies compared with hematopoietic malignancies (48, 49). In addition, although the IC_{50} for UM-SCC lines overlapped that of keratinocytes, clinically significant skin or mucosal toxicity of bortezomib other than mild rash or mucositis has not been observed in our study or even with higher doses used in major phase II clinical trials (8, 16, 17, 36–38, 47–49).

We next investigated proteasome-dependent effects of bortezomib in the paired UMSCC-11A and UM-SCC-11B lines to examine the hypothesis that differences in kinetics of proteasome inhibition and/or ubiquitination could contribute to the differential response and potentially serve as indicators of sensitivity. Our studies show that bortezomib inhibits the proteasome to a lesser extent and with a slower kinetics in UM-SCC-11A cells when compared with UM-SCC-11B cells (Fig. 4A), consistent with such a hypothesis. Previously, bortezomib-induced inhibition of proteasome activity was reported to peak in peripheral blood cells or tumor specimens 1 h after delivery of the drug (8, 28). However, we found bortezomib-induced proteasome inhibition reached its peak in HNSCC at about 4 h after delivery even *in vitro*, and the peak effect was sustained for ~8 h,[5] similar to observations in a murine SCC transplantation model (50). Consistent with these differences, accumulation of ubiquitinated proteins and the extent of inhibition of NF-κB (dependent on IκB ubiquitination and degradation; refs. 16, 17) after bortezomib treatment were significantly lower in UM-SCC-11A cells when compared with UM-SCC-11B cells (Fig. 4B). In addition, we observed that, at the lower dose of bortezomib (10^{-9} mol/L), the proteasome activity in UM-SCC-11A was stimulated instead of inhibited (Fig. 4A), suggesting the possibility that proteasome activity was modified by bortezomib-inducible mechanisms that remain to be defined. These differential effects of bortezomib and low-dose stimulation of proteasome activity observed in UM-SCC-11A and UM-SCC-11B cells could potentially occur upstream of or at the proteasome level possibly due to differences in cellular drug uptake or metabolism, ubiquitinases, or chaperones affecting stability or to basal and inducible levels of proteasome components (16–18), which warrant investigation in future studies.

In the past, investigations have been conducted to identify the molecular mechanisms underlying sensitivity of different cancers to bortezomib, particularly in multiple myeloma. Based on these studies, there remains controversy regarding if and how much of the anticancer effect of bortezomib is dependent on NF-κB activity. In multiple myeloma, NF-κB-dependent expression of interleukin-6, ICAM, and vascular endothelial growth factor by bone marrow stroma and endothelium has been implicated in response and resistance to bortezomib (51, 52), but such a microenvironment is not identical to that of HNSCC or other solid cancers, which arise outside the bone marrow. Further, we did not detect differences in other NF-κB-related genes such as Bcl-2 or Hsp27 implicated in intrinsic resistance of multiple myeloma (data not shown). Our data in UM-SCC cells, as well as others from some solid tumors, suggest that NF-κB activity is an important but not the only factor determining the anticancer effects of bortezomib (11, 19–29, 32–35). Previously, our laboratory showed that murine and human HNSCC exhibit increased constitutive NF-κB activation and that specific inhibition of NF-κB increases cell death (5–11). At concentrations that inhibit NF-κB activation, bortezomib was able to block cell proliferation and induce cell death in a panel of murine and human SCC cells from the skin and aerodigestive tract as well as tumorigenesis in murine HNSCC xenograft animal models (11). In addition, specific inhibition of NF-κB by an inducible IκBα signal phosphorylation mutant as well as bortezomib was associated with significantly reduced proinflammatory and proangiogenic cytokines, Gro-1, and vascular endothelial growth factor production *in vitro* and suppression of angiogenesis *in vivo* (10, 11). Furthermore, among nine UM-SCC cell lines screened in this study, UM-SCC-9 and UM-SCC-38 are the most resistant lines to bortezomib and exhibit relatively low constitutive NF-κB activity (Fig. 1B), whereas UM-SCC-11B is the most sensitive cell line and exhibits high basal NF-κB binding and reporter activity (refs. 6, 43 and this study; Z. Chen, data not shown). The inhibitory effect of bortezomib corresponded to differences in the extent of inhibition on NF-κB activity by the reporter gene assay (Fig. 5). In UM-SCC-11B cells, bortezomib induced a stronger and earlier

[5] Z. Chen, unpublished observation.

inhibition of NF-κB reporter activity (Fig. 5B); by contrast, in UM-SCC-11A cells, the NF-κB activity was stimulated early and less inhibited by the drug (Fig. 5A). Together, our present and previous data are consistent with the hypothesis that NF-κB is important but not the only determinant of bortezomib activity in HNSCC.

In addition to the differential effects of bortezomib on NF-κB activity, UM-SCC-11A cells, relative to UM-SCC-11B, showed significant enhancement of AP-1 reporter activity (Fig. 5*E* and *F*), another proproliferative and prosurvival factor often coactivated in HNSCC (6, 7). Consistent with the finding of constitutive activation of AP-1 identified in UM-SCC cell lines (6, 7), we have shown that a subset of the tumor cell lines, including UM-SCC-11A and UM-SCC-11B, overexpress gene clusters with an increased prevalence of predicted AP-1 binding motifs in their promoter region when compared with the binding frequencies of other gene promoters (41). Because AP-1 includes Jun/Fos family protein complexes (2, 3), and proteasome inhibitors can potentially activate AP-1 via decreased turnover of Jun/Fos, one mechanism potentially contributing to differences in AP-1 induction in HNSCC may be due to the greater accumulation of Jun/Fos available to accept signals from upstream signal pathways (18). Previously, our laboratory obtained evidence for aberrant activation of signal pathways upstream of AP-1, including the intermediate kinase pathways, MEK/mitogen-activated protein kinase (7), and the membrane growth factor receptors, such as interleukin-1 receptor (5), epidermal growth factor receptor (7, 44, 45), and hepatocyte growth factor/c-Met (53). Our experiments using inhibitors of mitogen-activated protein kinase pathway kinases JNK, p38, or MEK/ERK (Fig. 6; ref. 7) support the hypothesis that JNK and p38 are major pathways activating AP-1 and promoting proliferation of UM-SCC-11A following bortezomib treatment. This observation is supported by our phase I clinical investigation, where bortezomib alone significantly suppressed nuclear localization of the phosphorylated active form of the p65 subunit of NF-κB but not ERK, Jun, or STAT3 phosphorylation by immunohistochemistry in patients' tumor specimens (47). Our data are also consistent with more recent reports that blockage of mitogen-activated protein kinase pathways can significantly enhance cytotoxicity and apoptosis in hematopoietic malignancies (23–25, 34). p38, JNK, and c-Jun activation have been studied in multiple myeloma, and the effects of p38 pathway on bortezomib sensitivity in multiple myeloma (23–25, 34) are similar to HNSCC as described in this study. However, increased c-Jun and JNK activation was associated with cell apoptosis induced by bortezomib (22, 27) in multiple myeloma, which is opposite what we observed in HNSCC and presented in this article. Such differences in c-Jun and JNK functions could be tissue specific as suggested by Podar et al. (22). In HNSCC cells, activation of JNK and AP-1 pathways has been consistently related to proproliferative, antiapoptosis, and angiogenesis functions (7, 44, 45), which is different from observations drawn from multiple myeloma.

Based on this and previous studies, we have worked to develop biomarkers including the molecules involved in NF-κB and AP-1 pathways in our clinical trial with bortezomib combined with radiation therapy (8, 11, 47). We have obtained biopsies from a subset of HNSCC patients with accessible tumors both pretreatment and post-treatment taken 24 h after the initial bortezomib treatment but before the initiation of radiotherapy. The intensity of baseline NF-κB/Rel, ERK, STAT3 nuclear staining, apoptosis (TUNEL), and proliferation (Ki-67) was quantified by immunohistochemistry, and effects of bortezomib on phospho-RelA, RelB, c-Rel, p105/p50, p100/p52, phospho-ERK1/2, and phospho-STAT3 was evaluated (47). HNSCC tumor specimens showed increased baseline nuclear staining for all five NF-κB subunits, phospho-ERK1/2, and phospho-STAT3 when compared with normal mucosa. In biopsied tumor specimens obtained 24 h post-bortezomib from these patients, apoptosis was detected by TUNEL staining in association with inhibition of nuclear phospho-RelA subunit of NF-κB in three of four patients, but there was no inhibition or increase in staining of nuclear phospho-ERK1/2 and/or c-Jun in these patients who subsequently progressed and in a patient with activated nuclear phospho-ERK1/2 and c-Jun in the absence of NF-κB who showed no apoptosis or clinical response (8, 47). We conclude that the bortezomib dosage tested in this trial inhibits activation of subunits of the canonical NF-κB pathway; however, it did not block nuclear activation of the noncanonical NF-κB or other prosurvival signal pathways, such as ERK or Jun, which may contribute to early or delayed progression after partial responses observed in patients with HNSCC following bortezomib. The data from the clinical study are consistent with our findings in this study and are presented elsewhere (47).

In conclusion, distinct differences in sensitivity to bortezomib were observed in UM-SCC-11A and UM-SCC-11B cells, including in xenograft models (Figs. 1-3). Our data suggest that the mechanisms underlying these differences may exist at various levels of the regulation, from differences in the extent of proteasome inhibition to variable effects on NF-κB and AP-1 transcription factor activity (Figs. 4 and 5). We showed that bortezomib inhibited proteasome and NF-κB activities in UM-SCC-11A cells to a lesser extent when compared with UM-SCC-11B cells (Figs. 4 and 5), and increased AP-1 activity in UM-SCC-11A cells was observed after treatment with bortezomib (Fig. 5). Blockage of JNK and other mitogen-activated protein kinase activities could reduce AP-1 activity and synergize with bortezomib antitumor activity in UM-SCC-11A cells (Fig. 6). This preclinical study suggests that assays comparing the effects of bortezomib in pretreatment and post-treatment biopsies on proteasome activity, NF-κB and AP-1 signal activation, proliferation, and apoptosis could be useful to develop biomarkers for clinical trials of cancers, in which heterogeneous responses to bortezomib have been observed. These biomarkers could be relevant for determining optimal regimens for more effective therapy. Inhibition of JNK and other mitogen-activated

protein kinase pathways, which block AP-1 activity and enhance bortezomib antitumor effects, may be one such combination meriting further investigation.

Disclosure of Potential Conflicts of Interest

No potential conflicts of interest were disclosed.

Acknowledgments

We thank Millennium Pharmaceuticals for providing bortezomib for this study and Drs. Mark Rolfe and William Riordan for providing the proteasome activity assay protocol.

References

1. Aggarwal BB. Nuclear factor-κB: the enemy within. Cancer Cell 2004; 6:203 – 8.

2. Shaulian E, Karin M. AP-1 as a regulator of cell life and death. Nature Cell Biol 2002;4:E131 – 6.

3. Eferl R, Wagner EF. AP-1: a double-edged sword in tumorigenesis. Nat Rev Cancer 2003;3:859 – 68.

4. Van Waes C. Nuclear factor-κB in development, prevention, and therapy of cancer. Clin Cancer Res 2007;13:1076 – 82.

5. Allen CT, Ricker JL, Chen Z, Van Waes C. Role of activated nuclear factor-κB in the pathogenesis and therapy of squamous cell carcinoma of the head and neck. Head Neck 2007;29:959 – 71.

6. Ondrey FG, Dong G, Sunwoo J, et al. Constitutive activation of transcription factors NF-κB, AP-1, and NF-IL6 in human head and neck squamous cell carcinoma cell lines that express pro-inflammatory and pro-angiogenic cytokines. Mol Carcinog 1999;26:119 – 29.

7. Bancroft CC, Chen Z, Yeh J, et al. Effects of pharmacologic antagonists of epidermal growth factor receptor, PI3K and MEK signal kinases on NF-κB and AP-1 activation and IL-8 and VEGF expression in human head and neck squamous cell carcinoma lines. Int J Cancer 2002; 99:538 – 48.

8. Van Waes C, Chang AA, Lebowitz PF, et al. Inhibition of nuclear factor-κB and target genes during combined therapy with proteasome inhibitor bortezomib and reirradiation in patients with recurrent head-and-neck squamous cell carcinoma. Int J Radiat Oncol Biol Phys 2005;63: 1400 – 12.

9. Duffey DC, Chen Z, Dong G, et al. Expression of a dominant-negative mutant inhibitor-κBα of nuclear factor-κB in human head and neck squamous cell carcinoma inhibits survival, proinflammatory cytokine expression, and tumor growth *in vivo*. Cancer Res 1999;59:3468 – 74.

10. Loercher A, Lee TL, Ricker JL, et al. Nuclear factor-κB is an important modulator of the altered gene expression profile and malignant phenotype in squamous cell carcinoma. Cancer Res 2004;64:6511 – 23.

11. Sunwoo JB, Chen Z, Dong G, et al. Novel proteasome inhibitor PS-341 inhibits activation of nuclear factor-κB, cell survival, tumor growth, and angiogenesis in squamous cell carcinoma. Clin Cancer Res 2001;7:1419 – 28.

12. Druzgal CH, Chen Z, Yeh NT, et al. A pilot study of longitudinal serum cytokine and angiogenesis factor levels as markers of therapeutic response and survival in patients with head and neck squamous cell carcinoma. Head Neck 2005;27:771 – 84.

13. Allen C, Duffy S, Teknos T, Islam M, Chen Z, Albert PS, Wolf G, Van Waes C. Nuclear factor-κB-related serum factors as longitudinal biomarkers of response and survival in advanced oropharyngeal carcinoma. Clin Cancer Res 2007;13:3182 – 90.

14. Zhang PL, Pellitteri PK, Law A, et al. Overexpression of phosphorylated nuclear factor-κB in tonsillar squamous cell carcinoma and high-grade dysplasia is associated with poor prognosis. Mod Pathol 2005;18: 924 – 32.

15. Chung CH, Parker JS, Ely K, et al. Gene expression profiles identify epithelial-to-mesenchymal transition and activation of nuclear factor-κB signaling as characteristics of a high-risk head and neck squamous cell carcinoma. Cancer Res 2006;66:8210 – 8.

16. Adams J. The development of proteasome inhibitors as anticancer drugs. Cancer Cell 2004;5:417 – 21.

17. Adams J, Palombella VJ, Sausville EA et al. Proteasome inhibitors: a novel class of potent and effective antitumor agents. Cancer Res 1999; 59:2615 – 22.

18. Treier M, Staszewski LM, Bohmann D. Ubiquitin-dependent c-Jun degradation *in vivo* is mediated by the delta domain. Cell 1994;78:787 – 98.

19. An J, Sun Y, Fisher M, Rettig MB. Maximal apoptosis of renal cell carcinoma by the proteasome inhibitor bortezomib is nuclear factor-KB dependent. Mol Cancer Ther 2004;3:727 – 36.

20. Dai Y, Rahmani M, Grant S. Proteasome inhibitors potentiate leukemic cell apoptosis induced by the cyclin-dependent kinase inhibitor flavopiridol through a SAPK/JNK-and NF-κB-dependent process. Oncogene 2003;22: 7108 – 22.

21. Hipp MS, Urbich C, Mayer P, et al. Proteasome inhibition leads to NF-κB-independent IL-8 transactivation in human endothelial cells through induction of AP-1. Eur J Immunol 2002;32:2208 – 2.

22. Podar K, Raab MS, Tonon G, et al. Up-regulation of c-Jun inhibits proliferation and induces apoptosis via caspase-triggered c-Abl cleavage in human multiple myeloma. Cancer Res 2007;67:1680 – 8.

23. Tai YT, Fulciniti M, Hideshima T, et al. Targeting MEK induces myeloma cell cytotoxicity and inhibits osteoclastogenesis. Blood 2007; 110:1656 – 63.

24. Kojima K, Konopleva M, Samudio IJ, Ruvolo V, Andreeff M. Mitogen-activated protein kinase kinase inhibition enhances nuclear proapoptotic function of p53 in acute myelogenous leukemia cells. Cancer Res 2007; 67:3210 – 9.

25. Navas TA, Nguyen AN, Hideshima T, et al. Inhibition of p38a MAPK enhances proteasome inhibitor-induced apoptosis of myeloma cells by modulating Hsp27, Bcl-XL, Mcl-1 and p53 levels *in vitro* and inhibits tumor growth *in vivo*. Leukemia 2006;20:1017 – 27.

26. Johnson TR, Stone K, Nikrad M, et al. The proteasome inhibitor PS-341 overcomes TRAIL resistance in Bax and caspase 9-negative or Bcl-xL overexpressing cells. Oncogene 2003;22:4953 – 63.

27. Yang Y, Ikezoe T, Saito T, Kobayashi M, Koeffler HP, Taguchi H. Proteasome inhibitor PS-341 induces growth arrest and apoptosis of non-small cell lung cancer cells via the JNK/c-JUN/AP-1 signaling. Cancer Sci 2004;95:176 – 80.

28. Yu J, Tiwari S, Steiner P, Zhang L. Differential apoptotic response to the proteasome inhibitor bortezomib [Velcade, PS-341] in Bax-deficient and p21-deficient colon cancer cells. Cancer Biol Ther 2003;2:694 – 9.

29. Fribley A, Zeng Q, Wang CY. Proteasome inhibitor PS-341 induces apoptosis through induction of endoplasmic reticulum stress-reactive oxygen species in head and neck squamous cell carcinoma cells. Mol Cell Biol 2004;24:9695 – 704.

30. Williams S, Pettaway C, Song R, Papandreou C, Logothetis C, McConkey DJ. Differential effects of the proteasome inhibitor bortezomib on apoptosis and angiogenesis in human prostate tumor xenografts. Mol Cancer Ther 2003;2:835 – 43.

31. Nawrocki ST, Bruns CJ, Harbison MT, et al. Effects of the proteasome inhibitor PS-341 on apoptosis and angiogenesis in orthotopic human pancreatic tumor xenografts. Mol Cancer Ther 2002;1:1243 – 53.

32. Duan J, Friedman J, Nottingham L, Chen Z, Ara G, Van Waes C. Nuclear factor-κB p65 small interfering RNA or proteasome inhibitor bortezomib sensitizes head and neck squamous cell carcinomas to classic histone deacetylase inhibitors and novel histone deacetylase inhibitor PXD101. Mol Cancer Ther 2007;61:37 – 50.

33. Chauhan D, Li G, Shringarpure R, et al. Blockade of Hsp27 overcomes bortezomib/proteasome inhibitor PS-341 resistance in lymphoma cells. Cancer Res 2003;63:6174 – 7.

34. Hideshima T, Podar K, Chauhan D, et al. p38 MAPK inhibition enhances PS-341 (bortezomib)-induced cytotoxicity against multiple myeloma cells. Oncogene 2004;23:8766 – 76.

35. Minderman H, Zhou Y, O'loughlin KL, Baer MR. Bortezomib activity and *in vitro* interactions with anthracyclines and cytarabine in acute myeloid leukemia cells are independent of multidrug resistance mechanisms and p53 status. Cancer Chemother Pharmacol 2007;60:245 – 55.

36. Kondagunta GV, Drucker B, Schwartz L, et al. Phase II trial of bortezomib for patients with advanced renal cell carcinoma. J Clin Oncol 2004;22:3720 – 5.

37. Fanucchi MP, Fossella FV, Belt R, et al. Randomized phase II study of bortezomib alone and bortezomib in combination with docetaxel in previously treated advanced non-small-cell lung cancer. J Clin Oncol 2006;24:5025 – 33.

38. Alberts SR, Foster NR, Morton RF, et al. PS-341 and gemcitabine in patients with metastatic pancreatic adenocarcinoma: a North Central Cancer Treatment Group (NCCTG) randomized phase II study. Ann Oncol 2005;16:1654 – 61.

39. Van Waes C, Sunwoo JB, DeGraff W, Mitchell JB. Radiosensitization and proteasome inhibition. In: Adams J, editor. Cancer drug discovery and development: proteasome inhibitors in cancer therapy. Totowa (NJ): Humana Press; 2004. pp. 123 – 31.

40. Krause C, Carey T, Ott R, Hurbis C, McClatchey K, Regezi J. Human squamous cell carcinoma. Establishment and characterization of new permanent cell lines. Arch Otolaryngol 1982;107:703 – 10.

41. Yan B, Yang X, Lee TL, et al. Genome-wide identification of novel expression signatures reveal distinct patterns and prevalence of binding motifs for p53, NF-κB and other signal transcription factors in head and neck squamous cell carcinoma. Genome Biol 2007;8:R78.

42. Elliott PJ, Soucy TA, Pien CS, Adams J, Lightcap ES. Assays for proteasome inhibition. Methods Mol Med 2003;85:163 – 72.

43. Yu M, Yeh J, Van Waes C. Protein kinase casein kinase 2 mediates inhibitor-κB kinase and aberrant nuclear factor-κB activation by serum factor(s) in head and neck squamous carcinoma cells. Cancer Res 2006; 66:6722 – 31.

44. Lee TL, Yeh J, Van Waes C, Chen Z. Epigenetic modification of SOCS-1 differentially regulates STAT3 activation in response to interleukin-6 receptor and epidermal growth factor receptor signaling through JAK and/or MEK in head and neck squamous cell carcinomas. Mol Cancer Ther 2006;5:8 – 19.

45. Pernas FG, Allen CT, Winters ME, et al. Proteomic signatures of epidermal growth factor receptor and survival signal pathways correspond to gefitinib sensitivity in head and neck cancer. 99th Annual Meeting of AACR, San Diego CA, 2008 Apr 12-16.

46. Zhang X, Liu Y, Gilcrease MZ, et al. A lymph node metastatic mouse model reveals alterations of metastasis-related gene expression in metastatic human oral carcinoma sublines selected from a poorly metastatic parental cell line. Cancer 2002;95:1663 – 72.

47. Allen CT, Chang AA, Chen Z, et al. Bortezomib-induced apoptosis with limited clinical response is accompanied by inhibition of canonical but not alternative NF-κB subunits or other prosurvival signal pathways activated in head and neck cancer. Clin Cancer Res 2008. In press.

48. Russo A, Fratto ME, Bazan V, et al. Targeting apoptosis in solid tumors: the role of bortezomib from preclinical to clinical evidence. Exp Opin Ther Targets 2008;11:1571 – 86.

49. Hamilton AL, Eder JP, Pavlick AC, et al. Proteasome inhibition with bortezomib (PS-341): a phase I study with pharmacodynamic end points using a day 1 and day 4 schedule in a 14-day cycle. J Clin Oncol 2005;23: 6107 – 16.

50. Poff JA, Traughber B, Allen C, et al. Pulsed-high intensity focused ultrasound enhances apoptosis and growth inhibition of squamous cell carcinoma xenografts by proteasome inhibitor bortezomib. Radiology 2008. In press.

51. Hideshima A. Preclinical studies of novel targeted therapies. Hematol Clinics North Am 2007;21:1071 – 91.

52. Hideshima T, Akiyama M, Hayashi T, et al. Targeting p38 MAPK inhibits multiple myeloma cell growth in the bone marrow milieu. Blood 2003;101:703 – 5.

53. Dong G, Chen Z, Li ZY, Yeh NT, Bancroft CC, Van Waes C. Hepatocyte growth factor/scatter factor-induced activation of MEK and PI3K signal pathways contributes to expression of proangiogenic cytokines interleukin-8 and vascular endothelial growth factor in head and neck squamous cell carcinoma. Cancer Res 2001;61:5911 – 8.